Franciszek WITOS[1], Aneta OLSZEWSKA[2], Zbigniew OPILSKI[3]

22. LOCATION OF LEAKAGE IN METAL PIPELINES BY THE ACOUSTIC EMISSION METHOD USING MODELED AND NATURAL SOURCES

22.1. Introduction

Pipelines ensuring the transport of gaseous or liquid substances from one station to another or ensuring the proper course of production processes are a very important element in the economy. The basic issues enabling the continuity of their operation are leakage location and preventive testing of such pipelines. The methods of leak detection may be divided into two general categories [1]: direct (external) - the detection is done from outside the pipe through application of specialized sensors or visual observation and indirect (analytical, internal) - the detection is based on measurements and analysis of flow parameters (mainly pressure and fluid flow rate/velocity, sometimes temperature and density). Indirect methods may be divided into three categories: based on detection of the acoustic wave caused by the leak, based on mass balance concept, taking into consideration accumulation and analytical, and based on mathematical model and measurement of an object acquired from telemetry or SCADA system.

In the acoustic description, a leak is the leakage of a gas or liquid through a pipe wall containing the imperfection such as hole, crack or rupture. The leakage causes the imbalance pressure which is the source of the acoustic wave propagating in the pipeline. The recording of this wave and the analysis of its properties is the basis for acoustic leakage tests, which play a significant role in leakage testing [2, 3, 4].

The acoustic emission (AE) method has been successfully used for leakage testing in pipelines. Principles of conducting such research have been developed by Standards [5, 6]. Basic theoretical and experimental studies have been and are conducted with the use of two

[1] Department of Optoelectronics, Faculty of Electrical Engineering, Silesian University of Technology, Krzywoustego 2, 44-100 Gliwice, Poland, franciszek.witos@polsl.pl
[2] Department of Optoelectronics, Faculty of Electrical Engineering, Silesian University of Technology, Krzywoustego 2, 44-100 Gliwice, Poland, aneta.olszewska@polsl.pl
[3] Department of Optoelectronics, Faculty of Electrical Engineering, Silesian University of Technology, Krzywoustego 2, 44-100 Gliwice, Poland, zbigniew.opilski@polsl.pl

AE sensors with resonant frequency of 10-40 kHz mounted to the outside of the pipeline [7, 8]. There are also studies on buried pipes [9,10] and small leakage [8].

AE is also used for preventive testing of pipelines and then the purpose of the tests is to check the integrity of the pipeline, looking for possible sources of AE in the tested pipeline - these may be corrosion, micro-leaks, aging processes and others.

In the field of preventive testing of pipelines using the AE method, the authors have experience in conducting tests on 5 fragments of pipelines transporting crude oil/gasoline. This research was possible thanks to the fact that since 2015 the authors have AT level 2 certificates. Using these competences, the authors conducted tests of over twenty different objects such as pressure equipment and storage tanks with a strictly vertical axis [11]. The authors have been involved in AE research in various materials, objects and devices for over forty years, and for over twenty years they have been researching partial discharges (PD) in materials, objects and electrical devices [12-16]. These experiences were the basis for the construction of original measuring equipment dedicated to AE investigations [17, 18].

Currently, the authors are starting research to apply AE methods to locate leaks in metal pipelines. This paper presents a developed method for locating leaks in metal pipelines. The results of research carried out on a laboratory and real facility are presented. These tests were carried out on open-air pipelines, but the method can be applied to buried objects. For buried object in order to carry out measurements, it is necessary to expose the pipeline in two places, so that AE sensors are installed and measurements are first performed to ensure the determination of attenuation curves for two measurement paths containing two AE sensors and then carry out measurements in accordance with the proposed methodology. Finally recorded signals are analyzed giving the location of the leak source. Such research is of great application importance.

22.2. Measurement system

The tests were carried out using the Vallen AMSY-6 two-channel measurement system equipped with VS30 SIC 46dB AE sensors and VS150 RIC AE sensors [19].

VS150 RIC sensors are piezoelectric AE sensors with an integrated preamplifier with a gain of 34 dB. They are dedicated to testing the integrity of metallic pressure vessels, in particular to testing micro-leaks. The amplitude-frequency characteristic for this type of sensor is shown in Fig. 1a.

VS30-SIC-46dB sensors are piezoelectric AE sensors with an integrated preamplifier with a gain of 46 dB. They are dedicated to monitoring large objects or objects made of highly damping material, and in particular they can be used for testing leakage in gas pipelines and corrosion of metal structures. The amplitude-frequency characteristic for this type of sensor is shown in Fig. 1b.

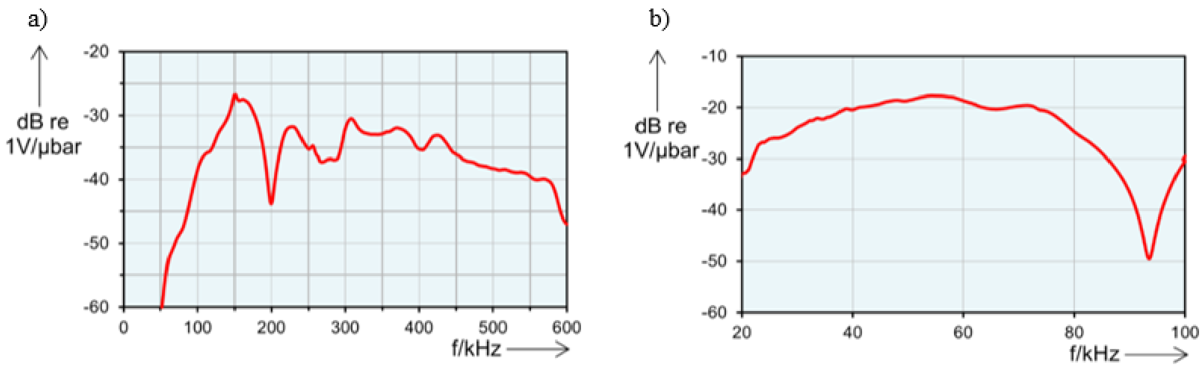

Fig. 1. Amplitude-frequency characteristics for: a) VS30-SIC-46dB sensors, b) VS150 RIC sensors
Rys. 1. Charakterystyki amplitudowo-częstotliwościowe dla: a) czujników VS30-SIC-46dB, b) czujników VS150 RIC

Vallen AMSY-6 is fully digital multi-channel AE measurement system. It consists of parallel measurement channels and the system front-end software which runs on an external PC. A measurement channel consists of an AE sensor, preamplifier and one channel of an ASIP-2 (dual channel acoustic signal processor). Each channel combines an analogue measurement section and a digital signal processing unit. AE features, such as time of the first threshold crossing (arrival time), risetime, duration, peak amplitude, energy and counts, are extracted by the ASIP-2. In parallel to the feature extraction, the complete waveform can be recorded by an optional transient recorder module.

Due to the necessity to record signals (from sources of various types generating signals of impulse or continuous type), two modes of signal registration can be used in the research giving either the "hit data" or "status data" type.

When using the "hit data" mode, pulses are recorded from the moment when the signal amplitude exceeds the threshold; when pretriggering is set, it is possible to record the signal from the point previously determined by pretriggering time, in all of them.

When using the "status data" mode, signals are recorded in packets lasting 0.1 seconds, which are combined into a continuous signal from start to stop, in all channels.

The use of different types of measurements requires to introduce a different set of parameters for the AMSY-6 measurement system each time.

22.3. The tested objects and the determined attenuation curves for the recorded signals from the Hsu-Nielsen tests

The research was carried out on the following facilities:

- pipeline A, diameter 90.0 cm, wall thickness 5.0 mm; natural gas pipeline,
- pipeline B, diameter 76.0 cm, wall thickness 4.0 mm; open pipeline,
- pipeline C, diameter 5.5 cm, wall thickness 2.5 mm; pipeline with propane-butane gas.

Each test began with the preparation of the test pipeline by removing the varnish and sanding the areas planned for the installation of AE sensors and the Hsu-Nielsen test site. Then, the signals from the sources generated during the Hsu-Nielsen tests were recorded. Hsu-Nielsen tests were performed at scheduled measuring points so as to allow determination of attenuation curves for the signals registered in different measuring channels.

Figures 2 - 5 show a fragment of pipeline A prepared for Hsu-Nielsen tests and examples of test results on pipeline A, as well as the determined attenuation curves for signals recorded in measurement lines with both types of sensors. The installation of the sensor has a fundamental and direct impact on the values of the measured quantities because the values of the recorded quantities are affected by the coupling layer (its size, shape and quality). Thus, the preparation of the surface by removing the varnish and sanding the areas planned for the mounting of the AE sensors and the Hsu-Nielsen test site (Fig. 2) is very important on account of measurement standard. Hsu-Nielsen sources [20, 21] are established standards as reproducible AE sources [21].

The recorded signal is a convolution of the signal generated during the Hsu-Nielsen test and the impulse response of the measuring system - therefore its Fourier transform is the product of the Fourier transform of the signal generated during the Hsu-Nielsen test and the transfer function of the circuit. In the performed tests of the transfer function of the AMSY-6 resonant measuring system, the amplitude-frequency characteristics (Fig. 3-4) are similar to the characteristics of the AE sensors used (Fig. 1). This fact is confirmed by the circumstance that the AMSY-6 measurement system (without sensors) is a wideband system. Fig. 5 and 6 show the attenuation curves for the signals recorded, respectively, in the measuring channels with an AE sensor of the VS150 SIC type (Fig. 5), and with the AR sensor of the VS30 SIC type (Fig. 6).

Fig. 2. A section of pipeline A prepared for Hsu-Nielsen tests with mounted AE sensors and with lines marked for Hsu-Nielsen tests at a distance of 3, 6, 8, 10 and 20 cm from the sensor's center, respectively

Rys. 2. Odcinek rurociągu A przygotowany do testów Hsu-Nielsena z zamontowanymi czujnikami EA i liniami oznaczonymi do testów Hsu-Nielsena w odległościach odpowiednio 3, 6, 8, 10 i 20 cm od środka czujnika

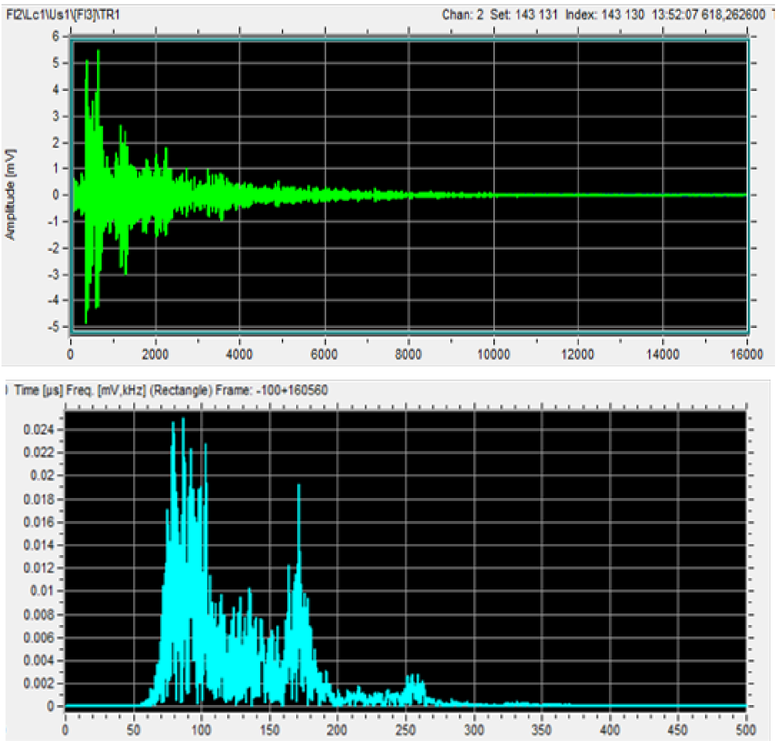

a)

b)

Fig. 3. a) signal recorded in the measuring channel with the AE sensor VS150 RIC during the Hsu-Nielsen test performed next to the sensor type, b) amplitude-frequency characteristic of signal

Rys. 3. a) sygnał rejestrowany w torze pomiarowym z czujnikiem AE VS150 RIC podczas testu Hsu-Nielsena wykonywanego obok typu czujnika, b) charakterystyka amplitudowo-częstotliwościowa sygnału

a)
b)

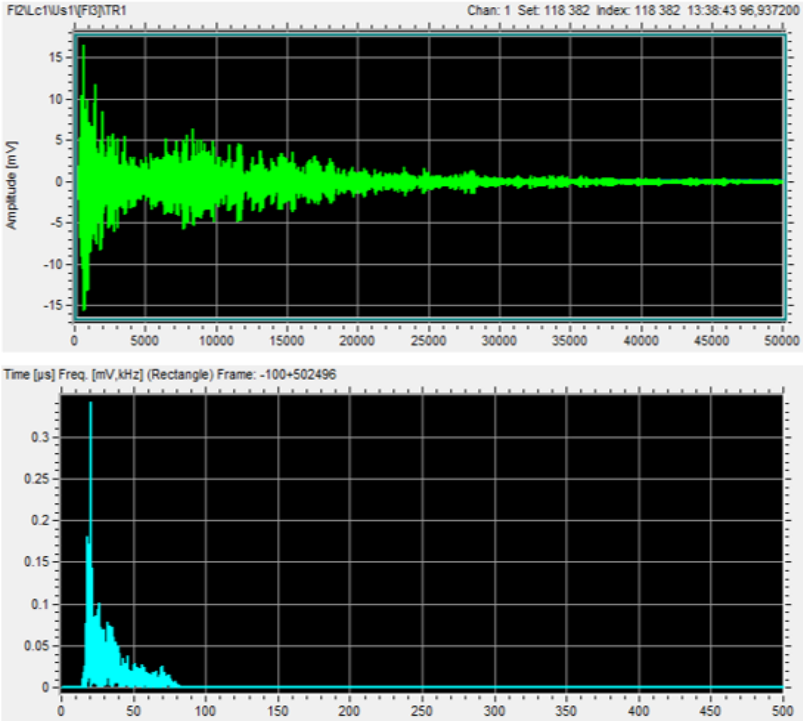

Fig. 4. a) signal recorded in the measuring channel with the AE sensor VS30-SIC-46dB during the Hsu-Nielsen test performed next to the sensor type, b) amplitude-frequency characteristic of signal

Rys. 4. a) sygnał rejestrowany w torze pomiarowym z czujnikiem AE VS30-SIC-46dB podczas testu Hsu-Nielsena wykonywanego obok typu czujnika, b) charakterystyka amplitudowo-częstotliwościowa sygnału

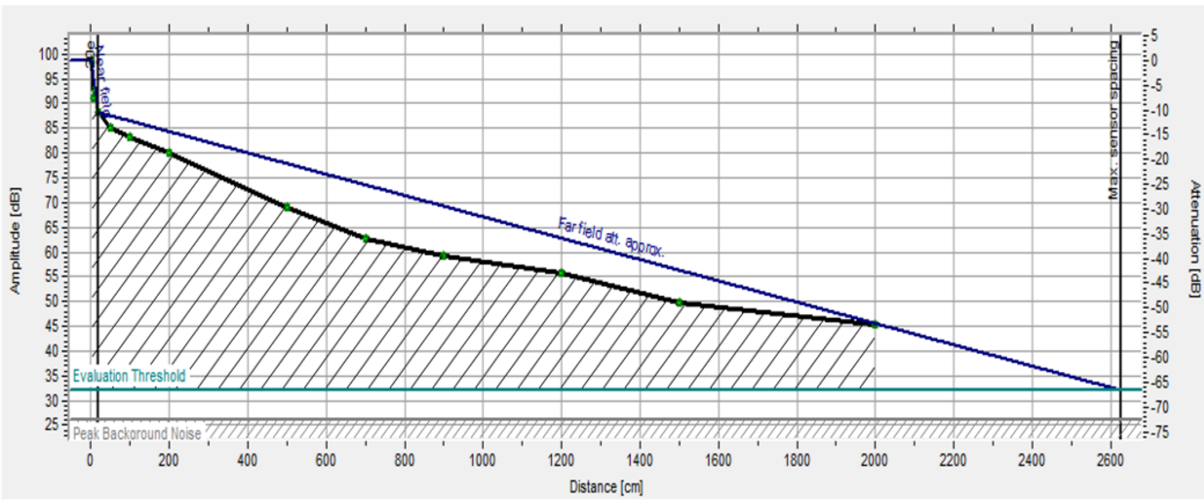

Fig. 5. Pipeline A, attenuation curve for the signals recorded in the measurement channel with AE sensor type VS150 RIC; the calculated maximum AE distance of the VS150 RIC sensors ensuring the location of the AE sources is 26.25 m

Rys. 5. Rurociąg A, krzywa tłumienia dla sygnałów rejestrowanych w kanale pomiarowym z czujnikiem AE typu VS150 RIC; obliczona maksymalna odległość AE czujników VS150 RIC zapewniająca lokalizację źródeł AE wynosi 26,25 m

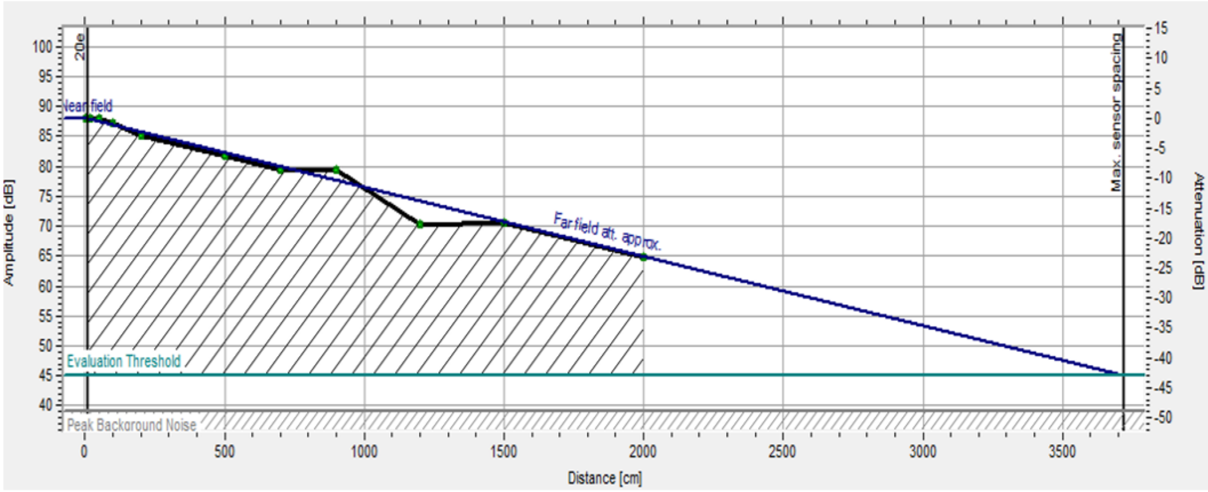

Fig. 6. Pipeline A, attenuation curve for the signals recorded in the measurement channel with AE sensor type VS30-SIC-46dB; the calculated maximum AE distance of the VS30-SIC-46dB sensors ensuring the location of the AE sources is 39.19 m

Rys. 6. Rurociąg A, krzywa tłumienia dla sygnałów rejestrowanych w kanale pomiarowym z czujnikiem AE typu VS30-SIC-46dB; obliczona maksymalna odległość AE czujników VS30-SIC-46dB zapewniająca lokalizację źródeł AE wynosi 39,19 m

The basic information resulting from the attenuation curves is the calculated maximum distance of the AE sensors ensuring the location of the AE sources. They are respectively: 2625 cm for sensors type VS150 SIC and 3719 cm for sensors type VS30 SIC. This also confirms the information shown in Fig. 1 that the main frequency band for sensors type VS150 SIC contains higher frequencies than the main frequency band for sensors type VS30 SIC. Additional information resulting from the detailed analysis of the attenuation curves are the following parameters: β_n - near field attenuation, β_f - far field attenuation and Δ_n - attenuation at 20e, $A_{H\text{-}N}$ - amplitude of signal registered during Hsu-Nielsen test, where e is the wall thickness of pipeline. The obtained results are summarized in Table 1.

Using the entered symbols and linear approximation in the far field, the amplitude of the $A_S(X)$ signal that will be registered by the sensor in the far field at the distance X from the position of the sensor during the Hsu-Nielsen tests is described by the formula:

$$A_S(X)=A_{H\text{-}N}-\Delta_n-\beta_f(X-20\mathrm{e}) \tag{1}$$

where: $A_S(X)$ - amplitude of the signal recorded by the sensor in the far field at the distance X from the position of the sensor during Hsu-Nielsen tests, $A_{H\text{-}N}$ - amplitude of the signal registered with the sensor during the Hsu-Nielsen test, Δ_n - attenuation at 20e, e - pipeline wall thickness, β_f - far field attenuation.

Table 1

Results of detailed analysis of attenuation curves

	VS150 SIC AE sensor				VS30 SIC AE sensor		
	max sensor spacing	near field attenuation	far field attenuation		max sensor spacing	near field attenuation	far field attenuation
	cm	dB/cm	dB/cm		cm	dB/cm	dB/cm
Pipe A	2625	0.624	0.022		3719	0.021	0.012

Using the entered symbols and linear approximation in the far field, the amplitude of the $A_S(X)$ signal that will be registered by the sensor in the far field at the distance X from the position of the sensor during the Hsu-Nielsen tests is described by the formula:

$$A_S(X)=A_{H\text{-}N}-\Delta_n-\beta_f(X-20\mathrm{e}) \tag{1}$$

where: $A_S(X)$ - amplitude of the signal recorded by the sensor in the far field at the distance X from the position of the sensor during Hsu-Nielsen tests, $A_{H\text{-}N}$ - amplitude of the signal registered with the sensor during the Hsu-Nielsen test, Δ_n - attenuation at 20e, e - pipeline wall thickness, β_f - far field attenuation.

22.4. Location of leakages in the form of modeled sources - the theoretical description

The theoretical description is related to the measurement situation shown in Fig. 7, in which the configuration of two AE sensors at a distance L from each other and the leak source located between the sensors is visible. The actual distances between the sensor and the leak source are described as L_1 (for the S1 sensor) and as L_2 (for the S2 sensor). If the amplitude of the signal generated in the source is marked as $A_{leakage}$, then the basis for locating the source of the leak is the system of equations presented in formulas (2) and (3)

$$\mathrm{A_{Si}}(L_i)=A_{leakage}-\Delta_{ni}-\beta_{fi}(L_i-20\mathrm{e_i}) \tag{2}$$

$$L_1+L_2=L \tag{3}$$

the index i in equation (2) takes the values 1 or 2 for sensors S1 or S2, respectively.

Solving for this system of equations gives the following values for L_1 and L_2:

$$L_1=(\beta_{f2}L+(A_{S2}(L_2)-A_{S1}(L_1))+(\Delta_{n2}-\Delta_{n1})+20(\beta_{f1}\mathrm{e}_1-\beta_{f2}\mathrm{e}_1))/(\beta_{f1}+\beta_{f2}) \tag{4}$$

$$L_2=(\beta_{f1}L-(A_{S2}(L_2)-A_{S1}(L_1))-(\Delta_{n2}-\Delta_{n1})+20(-\beta_{f1}\mathrm{e}_1+\beta_{f2}\mathrm{e}_1))/(\beta_{f1}+\beta_{f2}) \tag{5}$$

Fig. 7. Configuration of AE sensor S1 - Leakage source - AE sensor S2 used for the description of leakage source location by means of a measuring system with two measurement channels with sensors S1 and S2

Rys. 7. Konfiguracja: Czujnik EA S1 - Źródło wycieku - Czujnik EA S2 zastosowana przy opisie lokalizacji źródła wycieku za pomocą układu pomiarowego z dwoma kanałami pomiarowymi z czujnikami S1 i S2

22.5. Analysis of research results

22.5.1. Pipeline B

For testing the location of modeled leaks on pipeline B, a modeling source was designed and made (Fig. 8). The essence of the source's operation is to supply compressed air to the regulated valve and to regulate the compressed air stream flowing through this valve and hitting the pipeline. Compressed air is supplied from a pressure cylinder or a compressor via pressure pipes. The entire structure shown in Fig. 8a is balanced and can be suspended from the pipeline. The structure of the element enabling stable suspension on the pipeline is shown in Fig. 8b. Fig. 8c shows the source mounted on pipeline B.

During the tests, AE sensors of the VS150 RIC type were used, mounted at a distance of 10.54 m (distance $L_1 + L_2$ according to Fig. 7), and the leakage source was mounted at a distance of 8.00 m from the sensor S1 (distance L_1 according to Fig. 7). During operation of the AMSY-6 measurement system in the impulse mode, measurements were made on the basis of which the attenuation curves for both sensors were determined and the following parameters were determined: Δ_{n1} = 9.2 dB, β_{f1} = 0.021 dB/cm, Δ_{n2} = 9.1 dB, β_{f2} = 0.021 dB/cm.

Then the AMSY-6 measurement system was reinstalled for continuous operation. With the help of an adjustable valve, the amount of compressed air flowing through the valve and hitting the pipeline was determined and data was recorded in both measurement channels for about 10 seconds. Next, the volume of the compressed air stream flowing through the valve was increased and the data was again recorded in both measuring channels for about 10 seconds. In this way, the first measurement series was carried out in which the AE signals were recorded for ten different values of the amount of compressed air flowing through the valve. The measurement results are presented in Fig. 9, while Table 2 shows the analysis of the obtained results.

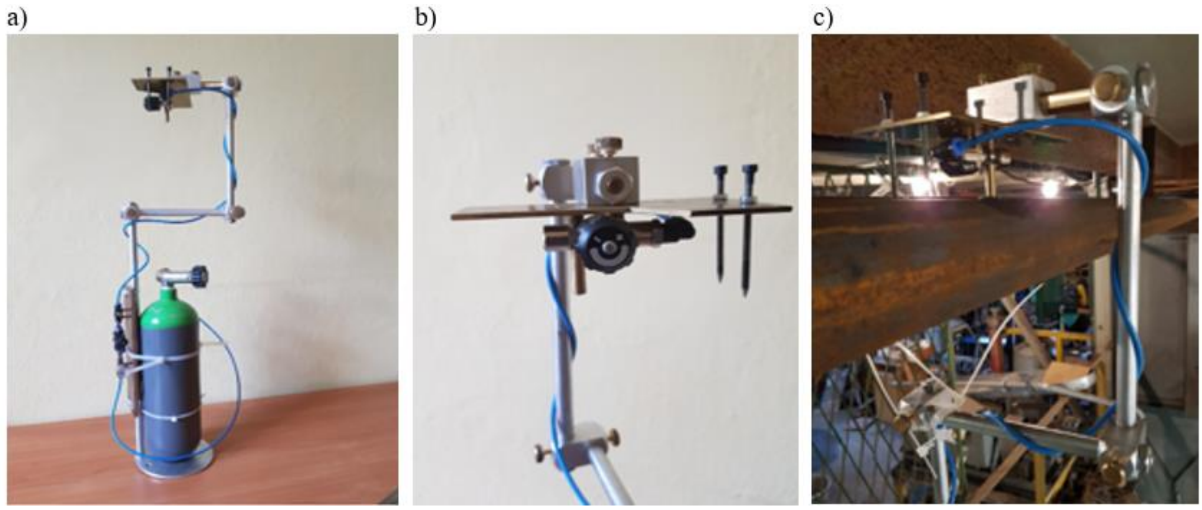

Fig. 8. Source for modeling leakages in the pipeline: a) general view of the source with a structure ensuring the use of compressed air cylinders (cooperation with a compressor is also possible), b) view of the used holder for the source adapted for stable mounting on the tested pipeline, c) source mounted on pipeline B

Rys. 8. Źródło do modelowania wycieków w rurociągu: a) widok ogólny źródła wraz z konstrukcją zapewniającą zastosowanie butli ze sprężonym powietrzem (możliwa jest również współpraca ze sprężarką), b) widok zastosowanego uchwytu źródła przystosowanego do stabilnego montażu na badany rurociąg, c) źródło zamontowane na rurociągu B

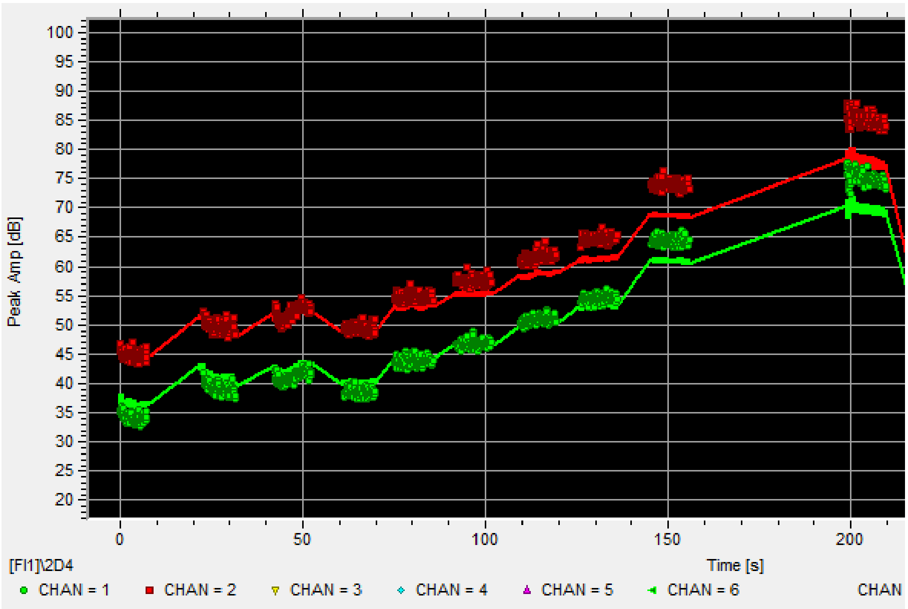

Fig. 9. Location of leakage source on pipeline B - results of first series of measurements. Registration of AE signals within two channels of AMSY-6 working in continuous mode with AE sensors VS150 RIC type. Positions in the configuration according to Fig. 7: 0 cm - AE sensor S1, 800 cm - Leakage source, 1054 cm - AE sensor S2

Rys. 9. Lokalizacja źródła wycieku na rurociągu B - wyniki pierwszej serii pomiarów. Rejestracja sygnałów EA w dwóch kanałach AMSY-6 pracujących w trybie ciągłym z czujnikami EA typu VS150 RIC. Pozycje w konfiguracji zgodnie z rys. 7: 0 cm - czujnik EA S1, 800 cm - źródło wycieku, 1054 cm - czujnik EA S2

Table 2

Location of leakage source on pipe B – first series of measurements

No.	Time	*A*(Ch2)	*A*(Ch1)	*A*(Ch2) −A(Ch1)	L_1	L_2	$L_{calc} - L_s$	$(L_{calc} - L_s)/L$
	s	dB	dB	dB	cm	cm	cm	%
1	4	44.9	33.9	11.0	788.9	265.1	11.1	1.4
2	25	49.4	39.3	10.1	767.5	286.5	32.5	4.1
3	45	50.8	40.6	10.2	769.9	284.1	30.1	3.8
4	50	53.3	42.0	11.3	796.0	258.0	4.0	0.5
5	65	49.5	38.9	10.6	779.4	274.6	20.6	2.6
6	80	54.9	43.8	11.1	791.3	262.7	8.7	1.1
7	95	57.6	47.0	10.6	779.4	274.6	20.6	2.6
8	115	61.5	50.9	10.6	779.4	274.6	20.6	2.6
9	130	65.0	54.6	10.4	774.6	279.4	25.4	3.2
10	150	74.2	63.8	10.4	774.6	279.4	25.4	3.2
11	205	85.6	75.3	10.3	772.2	281.8	27.8	3.5

The last two columns of Table 2 show the calculated values of the distance differences between the location of the source modeling the leakage and the location of the source obtained from the calculations. In the penultimate column, these differences are shown in centimeters, and in the last column they are the percentage differences with respect to the distance between the sensors. The analysis of the obtained location accuracy shows that the inaccuracy of the performed location is less than 4.2%, which should be considered a satisfactory result. The conducted tests have shown the functionality and stability of mounting the designed and manufactured source, which is a leak model.

The issue of whether the production of lower values of the amount of compressed air stream flowing through the valve will have an impact on the obtained results was also analyzed. For this purpose, a second series of measurements was performed. The measurement results are shown in Fig. 10, while Table 3 shows the results of the analysis of the properties of the recorded signals. The last column of Table 3 shows the calculated values of the differences between the position of the actual source of leakage Ls and the position of the source obtained from the L_{calc} calculations in relation to the distance between the sensors L (expressed as a percentage). Values for rows No. 2-11 show that the inaccuracy of the performed localization is less than 4.5%, which should be considered a satisfactory result. Regarding the result for the measurement No. 1, it should be stated that the inaccuracy is 13.0%, so it is much greater than the others. It should be added that in the measurement No. 1, there are large fluctuations in the amplitudes of A(Ch2) and A(Ch1) in the recorded signal and the mean values given in Table 3 have large standard deviations.

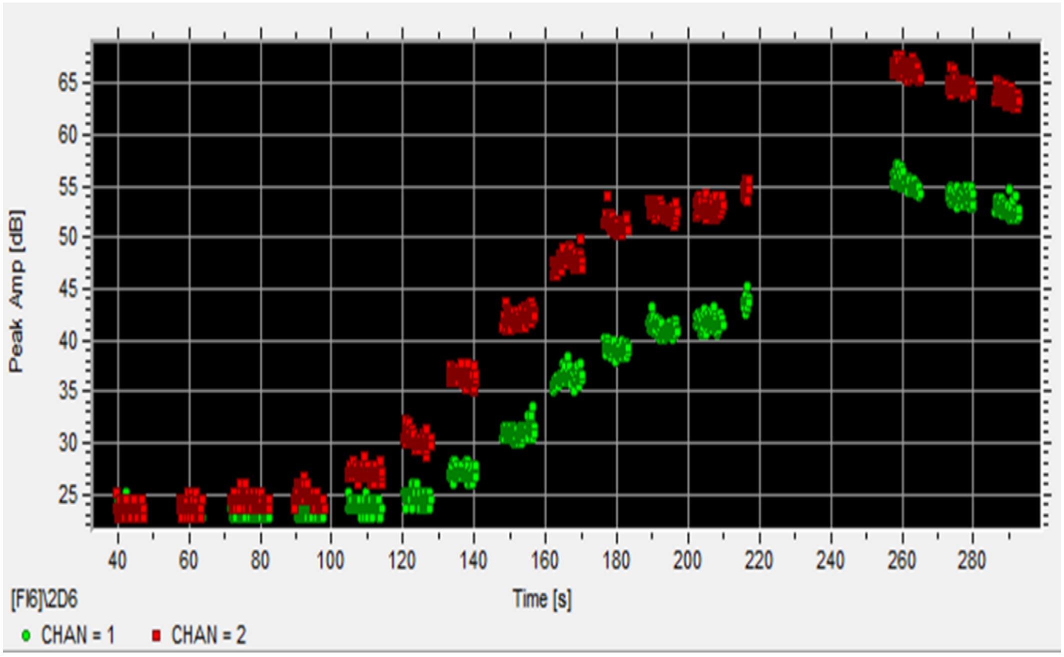

Fig. 10. Location of leakage source on pipe B - results of second series of measurements. Recording of AE signals within two channels of AMSY-6 working in continuous mode with AE sensors VS150 RIC type. Positions in the configuration according to Fig. 7: 0 cm - AE sensor S1, 800 cm - Leakage source, 1054 cm - AE sensor S2

Rys. 10. Lokalizacja źródła wycieku na rurze B - wyniki drugiej serii pomiarów. Rejestracja sygnałów AE w dwóch kanałach AMSY-6 pracujących w trybie ciągłym z czujnikami EA typu VS150 RIC. Pozycje w konfiguracji zgodnie z rys. 7: 0 cm - czujnik EA S1, 800 cm - źródło wycieku, 1054 cm - czujnik EA S2

Table 3

Location of leakage source on pipe B – second series of measurements

No.	Time	A(Ch2)	A(Ch1)	A(Ch2)–A(Ch1)	L_1	L_2	$L_{calc} - L_s$	$(L_{calc} - L_s)/L$
	s	dB	dB	dB	cm	cm	cm	%
1	124	30.5	24.5	7.0	696.1	357.9	103.9	13.0
2	137	36.9	27.2	10.3	765.1	288.9	34.9	4.4
3	152	42.3	31.3	11.0	791.3	262.7	8.7	1.1
4	166	47.7	36.5	11.2	796.1	257.9	3.9	0.5
5	180	51.1	38.9	12.2	819.9	234.1	19.9	2.5
6	193	52.8	40.7	12.1	817.5	236.5	17.5	2.2
7	206	52.9	41.8	11.0	791.3	262.7	8.7	1.1
8	216	54.6	43.6	11.1	793.7	260.3	6.3	0.8
9	261	66.3	54.9	11.4	800.8	253.2	0.8	0.1
10	276	64.8	54.2	10.6	781.8	272.2	18.2	2.3
11	289	63.4	52.3	10.9	788.9	265.1	11.1	1.4

This property of measurements has been confirmed during subsequent series, which means that sources of leakages with very low activity will be located with less accuracy. However, from a practical point of view, this limitation is not important as the essence of the location of the sources of leakage are high amplitude leaks, as they cause large economic losses.

The conducted laboratory tests are mainly of cognitive value, because from a practical point of view, it is important to locate the sources of leakages with a large amplitude, causing the outflow of a large amount of transported mass from the pipeline.

22.5.2. Pipeline C

After performing the tests on the B pipeline, indicating the functionality of the structure of the designed and constructed model of the leak source and confirming the possibility of locating the sources of leakages, two AE sensors in the configuration and the source of leaks between them based on the proposed description with solutions by expressions (4) and (5) the authors carried out research aimed at locating the source of the leak on a real object, which was a pipeline with propane-butane gas, i.e. on pipeline C. On pipeline C, the modeled source of gas leakage was a valve that could be set in 4 distinguishable positions:

a) MIN: minimum leakage,
b) MEDIUM: medium leak,
c) BIG: large leak,
d) MAX: maximum leakage.

During the tests, AE sensors were used, were mounted at a distance of 132.50 m (distance L1 + L2 according to Fig. 7), and the leakage source was mounted at a distance of 94.00 m from sensor S1 (distance L_1 according to Fig. 7). Due to the long distances, VS30 RIC AE sensors were used.

First, during the operation of the AMSY-6 measuring system in the impulse mode, measurements were made on the basis of which the attenuation curves for both sensors were determined and the following parameters were determined: Δ_{n1} = 1.2 dB, β_{f1} = 0.0107 dB/cm, Δ_{n2} = 1.2 dB, β_{f2} = 0.0200 dB/cm

Then the AMSY-6 measurement system was reinstalled for continuous operation. By means of an adjustable valve, various opening positions of the valve and the amount of propane-butane flowing out of the valve were recorded in both measurement channels for about 10 seconds. Leaks modeled in such a way are of practical importance as they cause an outflow of a significant mass transported by the pipeline. The results of the analysis of the recorded data in both measurement channels are presented in the form of amplitude distributions of the recorded signals (Fig. 11).

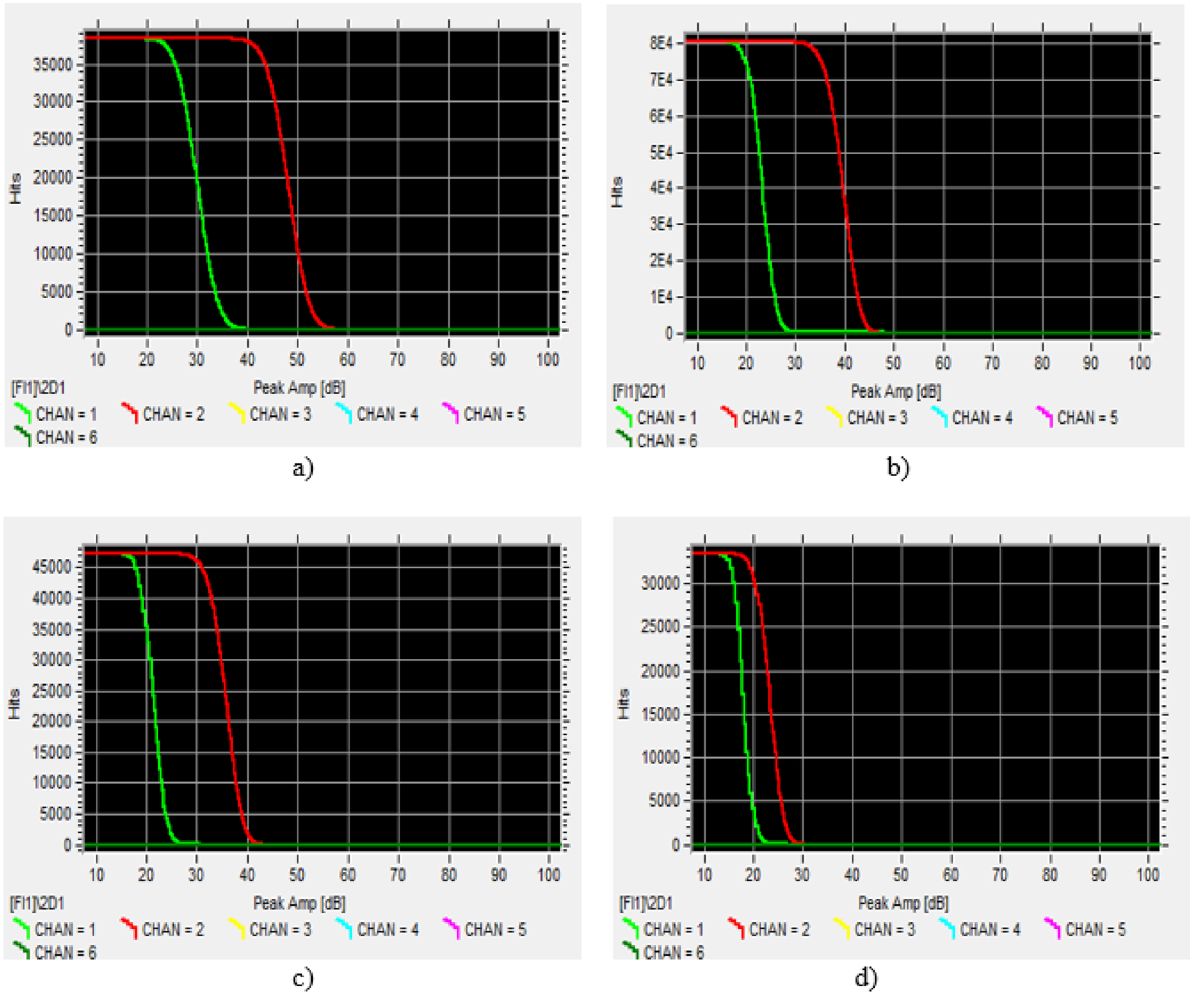

Fig. 11. Location of leakage source on pipeline C. Registration of AE signals within two channels of AMSY-6 working in continuous mode with AE sensors VS30 RIC type. Looms in the configuration according to Fig. 7: 0.00 m - AE sensor S1 (CH1), 94.00 m - Leakage source, 132.50 m - AE sensor S2 (CH2). Amplitude distributions of signals recorded in CH1 and CH2 measurement lines for a) MAX, b) LARGE, c) MEDIUM, d) MIN

Rys. 11. Lokalizacja źródła wycieku na rurociągu C. Rejestracja sygnałów EA w dwóch kanałach AMSY-6 pracujących w trybie ciągłym z czujnikami EA typu VS30 RIC. Wiązki w konfiguracji zgodnie z rys. 7: 0,00 m - czujnik EA S1 (CH1), 94,00 m - źródło przecieku, 132,50 m - czujnik EA S2 (CH2). Rozkłady amplitudy sygnałów rejestrowanych na liniach pomiarowych CH1 i CH2 dla a) MAX, b) LARGE, c) MEDIUM, d) MIN

The results of a detailed analysis of the properties of amplitude distributions and the results of leak source location are presented in Table 4. The last two columns of Table 4 show the calculated values of the difference in distance between the location of the leak source and the location of the source obtained from the calculations. In the penultimate column, these differences are shown in centimetres, and in the last column, they are relative percentages with respect to the distance between the sensors. The analysis of the obtained location inaccuracy shows that for all types of leakage, i.e. MAX, BIG, MEDIUM and MIN, it is less than 3%.

Table 4

Location of leakage source on pipe C

No.	Time	A(Ch2) $-A$(Ch1)	L_1	L_2	L_{calc} $-L_s$	$(L_{calc}$ $-L_s)/L$
	s	dB	m	m	cm	%
1	MAX	18.0	96.6	41.0	2.6	2.7
2	BIG	17.0	96.2	41.3	2.2	2.4
3	MEDIUM	15.0	95.6	42.0	1.6	1.7
4	MIN	6.0	92.6	44.9	1.4	1.4

This result should be considered satisfactory, the more so because it has its practical value and it is the simplest possible analysis of the recorded data. Currently, work is underway on the analysis of the signal in the frequency domain and with the use of the method of correlation of signals recorded simultaneously in two measurement channels.

22.6. Conclusions

The paper presents the application of the AE method for the location of leakage sources in metal pipelines. The application assumes:

- configuration of two AE sensors named S1 and S2 (located at a distance L) mounted on the pipeline and the leak source between the sensors,
- measurement of signals from Hsu-Nielsen tests and determination of the damping curves for the above-mentioned two measurement channels of the measuring system,
- recording of signals generated by an active source with two sensors that are elements of two measurement channels of the measurement system,
- analysis of the obtained results, in particular determining the distance sensor S1 - leak source and sensor S2 - leak source (according to the presented theoretical description) and ultimately the location of the leak source.

The method was verified in laboratory tests and on a real object.

For laboratory research a source has been designed and manufactured, the essence of which is to supply compressed air to the regulated valve and to regulate the stream flowing through the valve and hitting the pipeline. Laboratory tests were carried out using VS150 SIC type AE sensors mounted on the pipeline at a distance of 10.54 meters. The conducted tests showed the functionality and stability of mounting the designed and manufactured source, which is a leakage model, and confirmed the practical value of the proposed application of the AE method.

In the real object, the source of the leak was an adjustable valve located on the pipeline having four distinguishable valve opening positions. Laboratory tests were carried out using

AE sensors VS30 SIC mounted on the pipeline at a distance of 134.50 meters. The conducted tests showed the accuracy of the location not lower than 3%. Currently, works are carried out on the analysis of the signal in the frequency domain and with the use of the method of correlation of signals registered simultaneously in two measurement lines.

Bibliography

1. Turkowski M., Bratek A., Słowikowski M.: Methods and system of leak detection in long range pipelines. Journal of Automation, Mobile Robotics & Intelligent Systems 1(3), 2007, 39-46.
2. Adnan N.F, Ghazali M.F., Amin M.M., Hamat A.M.A.: Leak detection in gas pipeline by acoustic and signal processing - A review. 3rd International Conference of Mechanical Engineering Research (ICMER 2015), IOP Conference Series: Materials Science and Engineering, 12/22/2015, Vol. 100, 012013.
3. Chen B., Hei1 C., Luo M., Ho M.C., Song G: Pipeline two-dimensional impact location determination using time of arrival with instant phase (TOAIP) with piezoceramic transducer array. Smart Mater. Struct. 27, 2018, 105003 (12pp).
4. Meng L., Yuxing L., Wuchang W., Juntao F.: Experimental study on leak detection and location for gas pipeline based on acoustic method. Journal of Loss Prevention in the Process Industries 25, 2012, 90-102.
5. ASTM E1211/E1211M Standard Practice for Leak Detection and Location Using Surface-Mounted Acoustic Emission Sensors June 1, 2017.
6. Miller R.K., Pollock A.A., Watts D.J., Carlyle J.M., Tafuri A.N., Yezzi J.J.: A reference standard for the development of acoustic emission pipeline leak detection techniques. NDT&E International 32, 1999, 1-8.
7. Li S., Wen Y., Li P., Yang J., Yang L.: Leak detection and location for gas pipelines sing Acoustic Emission Sensors. 2012 IEEE International Ultrasonics Symposium, Oct. 2012, 957-960.
8. Yu, L. ; Li, S.Z.: Acoustic emission (AE) based small leak detection of galvanized steel pipe due to loosening of screw thread connection. Applied Acoustics 120 (2017), 85–89.
9. Anastaopoulus A., Kourousis D., Bollas K.: Acoutic emission leak detection of liquid filled buried pipeline. J. Acoustic Emission 27, 2009, 27-39.
10. Mostafapour A., Davoodi S.: A theoretical and experimental study on acoustic signals caused by leakage in buried gas-filled pipe. Appl. Acoust. 87, 2015, 1-8.
11. Witos. F.: Properties of amplitude distributions of acoustic emission signals generated in pressure vessel during testing. Arch. Acoust. 44(3), 2019, 493-503.
12. Olszewska A., Witos F.: Identification of acoustic emission signals originating from the core magnetization of power oil transformer. Arch. Acoust. 41(4), 2016, 798-812.

13. Witos F., Gacek Z.: Testing of partial discharges and location of their sources in generator coil bars by means of acoustic emission and electric methods, [in:] Acoustic Emission - Research and Applications, Sikorski W. [Ed.], Rijeka, InTech, 2013, 117-145.
14. Olszewska A., Witos F.: Location of partial discharge sources and analysis of signals in chosen power oil transformers by means of acoustic emission method. Acta Phys. Pol. A 122, 2012, 921-926.
15. Witos F., Olszewska A., Szerszeń G.: Analysis of properties characteristic for acoustic emission signals recorded on-line in power oil transformers. Acta Phys. Pol. A 120(4), 2011, 759-762.
16. Witos F., Gacek Z.: Application of the joint electro-acoustic method for partial discharge investigations within a power transformer. Eur. Phys. J., Spec. Top. 154(1), 2008, 239-247.
17. Witos F., Opilski Z., Szerszeń G., Setkiewicz M.: The 8AE-PD computer measurement system for registration and analysis of acoustic emission signals generated by partial discharges in oil power transformer. Metrol. Meas. Syst. 26(2), 2019, 404-418.
18. Witos F., Opilski Z., Szerszeń G., Setkiewicz M., Olszewska A., Duda D., Maźniewski K., Szadkowski M.: Calibration and laboratory testing of computer measuring system 8AE-PD dedicated for analysis of acoustic emission signals generated by partial discharges within oil power transformers. Arch. Acoust. 42(2), 2017, 297-311.
19. Vallen Systeme GmbH: www.vallen.de, 2021-02-03.
20. Boczar T., Lorenc M.: The repeatability and reproducibility of calibrating signals generated by Hsu-Nielsen method. J. Phys. IV France 129, 2005, 97-103.
21. Markus G., Sause R.: Investigation of pencil-lead breaks acoustic emission sources. J. Acoustic Emission, 29, 2011, 184-196.